OPEN

Development of Upright Computed Tomography With Area Detector for Whole-Body Scans

Phantom Study, Efficacy on Workflow, Effect of Gravity on Human Body, and Potential Clinical Impact

Masahiro Jinzaki, MD, PhD, Yoshitake Yamada, MD, PhD,* Takeo Nagura, MD, PhD,† Takehiro Nakahara, MD, PhD,* Yoichi Yokoyama, MD,* Keiichi Narita, MD,* Naomichi Ogihara, PhD,‡ and Minoru Yamada, PhD**

Objectives: Multiple human systems are greatly affected by gravity, and many disease symptoms are altered by posture. However, the overall anatomical structure and pathophysiology of the human body while standing has not been thoroughly analyzed due to the limitations of various upright imaging modalities, such as low spatial resolution, low contrast resolution, limited scan range, or long examination time. Recently, we developed an upright computed tomography (CT), which enables whole-torso cross-sectional scanning with 3-dimensional acquisition within 15 seconds. The purpose of this study was to evaluate the performance, workflow efficacy, effects of gravity on a large circulation system and the pelvic floor, and potential clinical impact of upright CT.

Materials and Methods: We compared noise characteristics, spatial resolution, and CT numbers in a phantom between supine and upright CT. Thirty-two asymptomatic volunteers (48.4 ± 11.5 years) prospectively underwent both CT examinations with the same scanning protocols on the same day. We conducted a questionnaire survey among these volunteers who underwent the upright CT examination to determine their opinions regarding the stability of using the pole throughout the acquisition (closed question), as well as safety and comfortability throughout each examination (both used 5-point scales). The total access time (sum of entry time and exit time) and gravity effects on a large circulation system and the pelvic floor were evaluated using the Wilcoxon signed-rank test and the Mann-Whitney *U* test. For a large circulation system, the areas of the vena cava and aorta were evaluated at 3 points (superior vena cava or ascending aorta, at the level of the diaphragm, and inferior vena cava or abdominal aorta). For the pelvic floor, distances were evaluated from the bladder neck to the pubococcygeal line and the anorectal junction to the pubococcygeal line. We also examined the usefulness of the upright CT in patients with functional diseases of spondylolisthesis, pelvic floor prolapse, and inguinal hernia.

Results: Noise characteristics, spatial resolution, and CT numbers on upright CT were comparable to those of supine CT. In the volunteer study, all volunteers answered yes regarding the stability of using the pole, and most reported feeling safe (average rating of 4.2) and comfortable (average rating of 3.8) throughout the upright CT examination. The total access time for the upright CT was significantly reduced by 56% in comparison with that of supine CT (upright: 41 ± 9 seconds vs supine: 91 ± 15 seconds, $P < 0.001$). In the upright position, the area of superior vena cava was 80% smaller than that of the supine position (upright: 39.9 ± 17.4 mm^2 vs supine: 195.4 ± 52.2 mm^2, $P < 0.001$), the area at the level of the diaphragm was similar (upright: 428.3 ± 87.9 mm^2 vs supine: 426.1 ± 82.0 mm^2, $P = 0.866$), and the area of inferior vena cava was 37% larger (upright: 346.6 ± 96.9 mm^2 vs supine: 252.5 ± 93.1 mm^2, $P < 0.001$), whereas the areas of aortas did not significantly differ among the 3 levels. The bladder neck and anorectal junction significantly descended (9.4 ± 6.0 mm and 8.0 ± 5.6 mm, respectively, both $P < 0.001$) in the standing position, relative to their levels in the supine position. This tendency of the bladder neck to descend was more prominent in women than in men (12.2 ± 5.2 mm in women vs 6.7 ± 5.6 mm in men, $P = 0.006$). In 3 patients, upright CT revealed lumbar foraminal stenosis, bladder prolapse, and inguinal hernia; moreover, it clarified the grade or clinical significance of the disease in a manner that was not apparent on conventional CT.

Conclusions: Upright CT was comparable to supine CT in physical characteristics, and it significantly reduced the access time for examination. Upright CT was useful in clarifying the effect of gravity on the human body: gravity differentially affected the volume and shape of the vena cava, depending on body position. The pelvic floor descended significantly in the standing position, compared with its location in the supine position, and the descent of the bladder neck was more prominent in women than in men. Upright CT could potentially aid in objective diagnosis and determination of the grade or clinical significance of common functional diseases.

Key Words: multidetector computed tomography, standing, posture, upright, vena cava, vein, pelvic floor, spondylolisthesis, bladder prolapse, inguinal hernia

(*Invest Radiol* 2020;55: 73–83)

Humans spend most of their day in an upright position, and although many disease symptoms are more remarkable in a standing position versus supine position, there are currently very few methods to analyze the effects of gravity on pathophysiology and anatomical structures throughout the upright human body. X-ray examination can provide images of a subject in a standing position[1]; however, it is a projection image, rather than a cross-sectional image. Cone beam computed tomography (CT) can provide cross-sectional images in a standing position; however, the resulting soft tissue information is insufficient due to its low contrast.[2,3] Furthermore, scan range is often limited because of its narrow bore size[4–6]; however, a new type of cone beam CT has recently been developed that enables imaging of central joints, such as the spine.[7] Thus, its clinical applications remain limited to high-contrast tissues, such as dentition or extremities.[2,3]

Received for publication April 26, 2019; and accepted for publication, after revision, July 1, 2019.

From the Departments of *Diagnostic Radiology, and †Orthopedic Surgery, Keio University School of Medicine, Tokyo; and ‡Department of Mechanical Engineering, Faculty of Science and Technology, Keio University, Yokohama, Japan.

Conflicts of interest and sources of funding: This study was supported by Canon Medical Systems. This study was supported by Japan Society for the Promotion of Science (JSPS KAKENHI: grant number JP17H04266), Uehara Memorial Foundation, and Canon Medical Systems (Otawara, Japan). Masahiro Jinzaki has received a grant from Canon Medical Systems. Canon Medical Systems has loaned the upright computed tomography machine to Keio University. However, Canon Medical Systems is not involved in the design and conduct of the study; in the collection, analysis, and interpretation of the data; and in the preparation, review, or approval of the manuscript. All other authors have no relationships with industry or other entities.

Supplemental digital contents are available for this article. Direct URL citations appear in the printed text and are provided in the HTML and PDF versions of this article on the journal's Web site (www.investigativeradiology.com).

Correspondence to: Masahiro Jinzaki, MD, PhD, Department of Radiology, Keio University School of Medicine, 35 Shinanomachi, Shinjuku-ku, Tokyo, 160-8582, Japan. E-mail: jinzaki@rad.med.keio.ac.jp.

ISSN: 0020-9996/20/5502–0073
DOI: 10.1097/RLI.0000000000000603

FIGURE 1. Upright CT machine and tools for safety. Our upright CT system enables up-and-down movements with a transverse 320 row-detector gantry. A, Gantry in the up position. B, Gantry in the down position. C, Knee-high acrylic wall encircling the body. D, Pole to lightly support the back of the patient.

Computed tomography has provided cross-sectional images of the whole body, including soft tissue in a supine position, since its initial development in 1972.[8] At that point, there were plans to develop this modality for use in the standing position; however, this was not realized due to difficulties associated with keeping subjects in a standing position for the length of time needed to obtain images of the entire body. In the late 1990s, upright magnetic resonance imaging (MRI) with an open configuration was introduced, which enabled the visualization of cross-sectional images in the upright position with high-contrast soft tissue images.[9–11] However, the strength of the magnetic field is low (0.2 to 0.6 T) in this method, compared with that of widely used conventional MRI (1.5 T or 3.0 T); thus, signal-to-noise ratio, contrast, and resolution are lower than those of conventional MRI.[12,13] As a result, longer examination time is necessary to achieve appropriate image quality, which causes motion artifacts in the standing position.[13] Overall, the effects of gravity on the entire body, as well as on its internal systems, have not been well evaluated; the effects of gravity on the pelvic floor have been evaluated primarily in the sitting position, rather than the standing position.[10] Furthermore, due to the inability to obtain 3-dimensional imaging, there is difficulty in using upright MRI to evaluate small structures, such as the canal and lateral recess of the spine, when sections or image planes are not accurately matched to the anatomical structure.[12]

Currently, 0.5-second scanning per rotation is clinically available in CT, which enables 3-dimensional imaging of the torso in less than 15 seconds using 64-row or 80-row detector CT. In addition, with the reemergence of reconstruction techniques in 2009,[14] the radiation dose necessary for CT has dramatically decreased.[15] Currently, chest CT images are available at a dose of 0.12 mSv, nearly equal to that of a simple chest x-ray examination.[16] As the use of CT has resulted in shorter scanning times, fewer radiation doses, and an ability to obtain functional information, we proposed and developed an upright CT scanner for the entire body, in conjunction with Toshiba Medical Systems (now known as Canon Medical Systems).

The purpose of our study was to (1) evaluate the physical performance of upright CT using a phantom; (2) evaluate the workflow efficacy

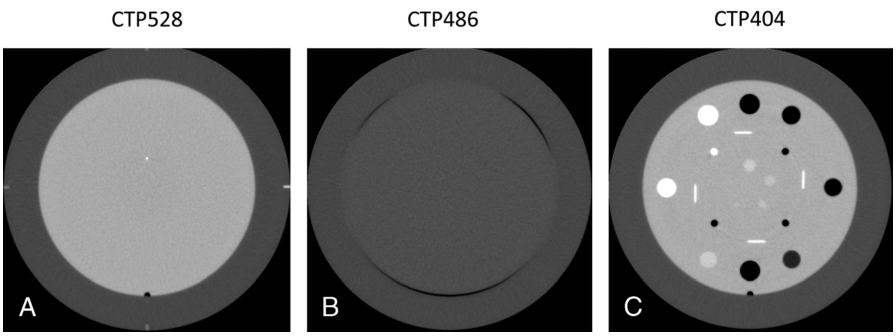

FIGURE 2. CT images of Catphan 504 consisted of CTP528, CTP486, and CTP404. A, CTP528 for MTF (modulation transfer function) contains a bead point source. B, A region of interest (ROI) of 100 cm^2 (256 × 256 pixels) was placed on the center of the image of CTP486 for NPS (noise power spectrum). C, CTP404 for CT number measurements contains inserts made of air, polymethylpentene (PMP), low-density polyethylene (LDPE), polystyrene, acrylic, Delrin, and Teflon.

TABLE 1. Scanning Parameters of Phantom Study

	Phantom Component	kVp	mA	Beam Collimation, mm	Helical Pitch	Noise Index for 5-mm Slice Thickness	dFOV, mm	Recons Kernel	Slice Thickness/Slice Interval, mm	Analysis Method
MTF	CTP528	120	750	80 × 0.5	0.813	3	50	FC13	1/0.1	Fourier transform of the PSF
NPS	CTP486	120	500	80 × 0.5	0.813	3	200	FC13	5/5	Radial frequency method
CT number	CTP404	120	750	80 × 0.5	0.813	3	200	FC13	5/5	Hounsfield Unit

MTF indicates modulation transfer function; NPS, noise power spectrum; dFOV, display field of view; PSF, point spread function; FC13, standard kernel without beam hardening correction; CT, computed tomography.

of upright CT and the effects of gravity on a large circulation system and the pelvic floor by employing volunteers, both of which have been poorly evaluated in the standing position; and (3) describe the potential clinical impact of upright CT using patient data.

MATERIALS AND METHODS

Constitution of Upright CT

Our upright CT system is capable of up-and-down movements of a transverse 320 row-detector gantry (isotropic 0.5 mm in detector size), with a 0.275-second gantry rotation speed, maximum vertical speed of 100 mm/s, and a 1200 view, at optimal performance (Fig. 1, see Supplementary Video 1, Supplemental Digital Content 1, http://links.lww.com/RLI/A473, which demonstrates the up-and-down movements of upright CT). The gantry for this device includes a stand that supports the rotary on either side; it also contains the linear motion rail and ball screw to move the scanner up and down. To achieve the up-down motion of the heavy rotary with a high-speed, high-precision rotation with the least amount of vibration for reduction of motion artifacts, and accurate horizontal position of the gantry during rotation, implemented technologies included a high-speed movement control mechanism, a horizontal compensation mechanism, and a rotating part structure with high rigidity. The maximum and minimum scan heights relative to the floor were 175 cm and 40 cm, respectively. The minimally required footprint of upright CT would be two thirds of that of conventional 320 row-detector CT.

For safety during scanning, the area cover was equipped with a pinch prevention mechanism and contact interlock control mechanism. A knee-high acrylic wall encircling the body was also added to prevent falls. Furthermore, to stabilize patients when standing, a back support pole was included (Fig. 1). The pole is 2.3 m long and made of carbon; it is mounted between the floor and top of the system. The mounting position can be adjusted based on the patient's bodily dimensions or the scan conditions.

Phantom Study

We evaluated the physical performance using the Catphan 504 phantom (The Phantom Laboratory, Salem, NY) to determine whether image quality degradation was present, by adapting the up-down moving system in upright CT. This phantom included CTP528, CTP486,

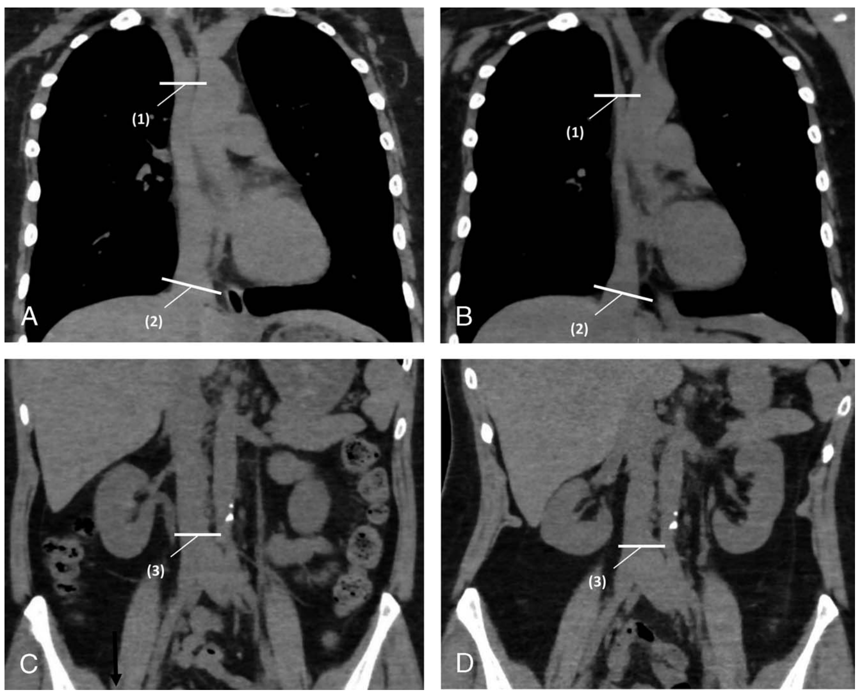

FIGURE 3. Measured points on the vena cava. Each coronal reformatted unenhanced CT image demonstrates the 3 points where the area size and flattening ([major axis – minor axis]/major axis) measurements of the vena cava were performed. These points include (1) directly below the junction of the bilateral cephalic veins, (2) at the height of the diaphragm, and (3) directly above the junction of bilateral common iliac veins. A, Supine position (thoracic). B, Upright position (thoracic). C, Supine position (abdominal). D, Upright position (abdominal).

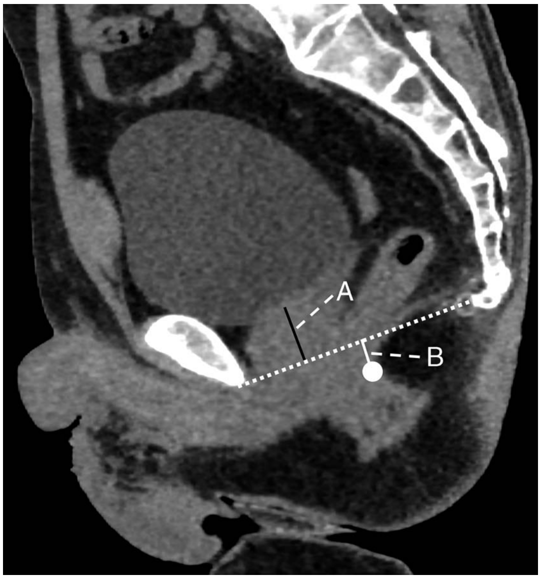

FIGURE 4. Measurement of the pelvic floor. A, From bladder neck to PC line. B, From anorectal junction to PC line. Dotted line indicates PC line (pubococcygeal line); black line, bladder neck; white line, anorectal junction.

and CTP404 components (Fig. 2). We compared spatial resolution, noise characteristics, and CT numbers between the upright CT and a conventional 320-detector row CT scanner (Area detector CT: Aquilion ONE Vision edition, Canon Medical Systems, Otawara, Japan). We examined spatial resolution by analyzing the modulation transfer function (MTF) in xy-plane and in z-axis using the CTP528.[17–19] We examined noise characteristics by analyzing the noise power spectrum (NPS) in-plane using the CTP486.[20–22] Lastly, we examined CT numbers using the CTP404. The scanning protocol and analysis method are shown in Table 1. To improve the accuracy of data, 5 scans were performed with the same table position in all data sets, and a total of 5 curves were averaged for each CT scanner. All data were analyzed by using ImageJ (US National Institutes of Health, Bethesda, MD).

Volunteer Study and Patient Study

We conducted a prospective pilot study in which healthy volunteers were recruited to investigate the effects of gravity on a large circulation system and the pelvic floor. We also performed a second pilot study of patients with functional disease. The volunteer and patient studies were approved by the ethical committee of our institute, and written consent was obtained from all participants (UMIN Clinical Trials Registry [UMIN-CTR]: UMIN000026586, UMIN000026953, UMIN000030386).

There were 32 consecutive asymptomatic volunteers from a volunteer recruitment company, consisting of 16 men and 16 women. Four men and 4 women, from the third, fourth, fifth, and sixth decades of life, were enrolled in this study. To evaluate normal whole-body anatomy, volunteers with a history of smoking, diabetes, hypertension, dyslipidemia, awareness of dysuria, or those who had undergone a surgical operation or were currently undergoing treatment were excluded.

The volunteers prospectively underwent both upright CT and conventional 320-detector row CT (Aquilion ONE, Canon Medical Systems) on the same day for head and body trunk, separately. Head scans were performed in the sitting position in a chair, and body trunk scans were performed in the standing position using the pole, as well as with the aid of a knee-high acrylic wall encircling the body. The scan lengths for the head and body trunk were adjusted to be identical between supine and upright CT scans. Only data for the body trunk were analyzed in this study. For the body trunk, scanning was performed at 120 kVp, 0.5 seconds of gantry rotation, helical scan mode (80-row detector), with a noise index of 15 and helical pitch of 0.8 for the abdominal CT. The calculated acquisition time was 13.7 ± 0.6 seconds, and the field of view and average scan length were 50 cm and 833.4 mm (range, 770–900 mm), respectively. Image reconstruction was performed using Adaptive Iterative Dose Reduction 3D. Supine CT was performed first, followed by upright CT. The effective dose estimate for the body trunk was 9.3 ± 2.2 mSv for supine CT and 8.9 ± 2.0 mSv for upright CT.

We conducted a questionnaire survey at the end of the examinations of the body trunk regarding stability when using the pole throughout the acquisition, as well as safety and comfortability throughout the examination. The question regarding stability was a closed question: volunteers answered "yes" if they felt sufficient stability, and "no" if they felt any instability. Questions regarding safety and comfortability were 5-point scales, where 5 indicates "totally agree" (very safe or very comfortable) and 1 indicates "totally disagree" (dangerous or uncomfortable).

We measured the examination time for the body trunk scan. The total examination time included (1) time taken for the patient to enter the room and be positioned for the scan (entry time); (2) time taken to acquire 2 scout scans of front and lateral views, as well as 1 main scan (total operation time); and (3) time taken for the patient to disengage and exit the room (exit time). The "total access time" refers to the sum of the entry and exit times. To maintain consistency, times were measured by the same radiographer for all examinations. We compared total access time and total operation time between supine and upright CT scans.

Measurements of area size and flattening ([major axis – minor axis]/major axis) of the vena cava were manually performed on orthogonal

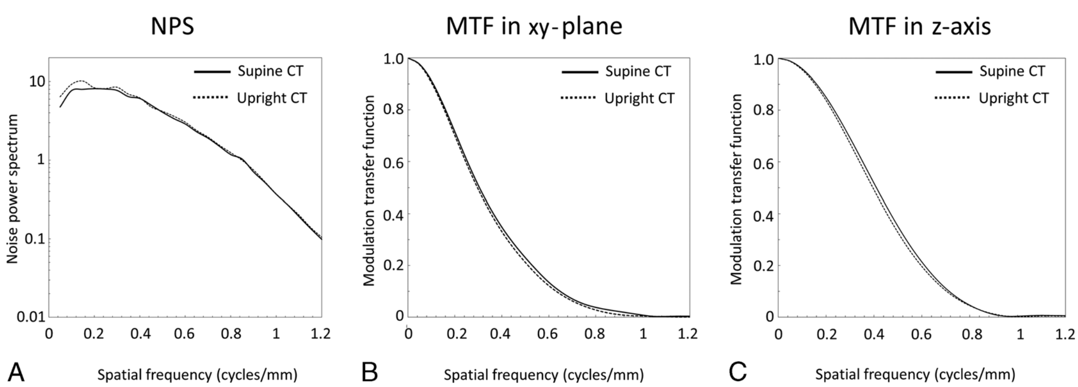

FIGURE 5. Noise power spectrum and MTF curves of upright CT and supine CT. Both noise characteristics (noise power spectrum) and spatial resolution (modulation transfer function) of upright CT were comparable to those of conventional CT. A, NPS (noise power spectrum). B, MTF (modulation transfer function) in xy-plane. C, MTF in *z*-axis.

TABLE 2. CT Numbers Measured in Upright CT and Described in Catphan 504 Manual

	Air	PMP	LDPE	Polystyrene	Acrylic	Delrin	Teflon
Average CT number, HU							
Conventional	−987.2	−178.4	−88.4	−34.7	123.4	344.2	942.6
Upright	−987.0	−178.2	−88.2	−33.2	124.2	344.2	942.2
Range in catphan manual, HU	−1046:−986	−220:−172	−121:−87	−65:−29	92:137	344:387	941:1060

CT indicates computed tomography; PMP, polymethylpentene; LDPE, low-density polyethylene.

cross-sectional areas at 3 different points using a commercially available workstation (Vitrea, Canon Medical Systems): superior vena cava (SVC) directly below the junction of bilateral cephalic veins, a point at the height of the diaphragm, and inferior vena cava (IVC) directly above the junction of the bilateral common iliac veins (Fig. 3). These measurement points of SVC and IVC were selected because the change in area seemed remarkable. Measurements of the aorta were made at the sinotubular junction (ascending aorta), a point at the height of the diaphragm (identical to that measured for the vena cava), and a point directly above the bifurcation point of the bilateral common iliac artery. The distances from the bladder neck to the pubococcygeal line (PC line)[23] and from the anorectal junction (defined as the posterior aspect of the puborectalis muscle sling) to the PC line were measured for the pelvic floor[24] (Fig. 4).

For all 32 volunteers, the first vessel diameter measurement was performed by a cardiovascular radiologist with 12 years of experience and the first pelvic floor measurement was performed by a genitourinary radiologist with 10 years of experience. A second measurement of 16 initial volunteers was performed by the same reader to assess intraobserver agreement 1 month after the first reading. To assess interobserver agreement, vessel diameter measurements of 16 initial volunteers were performed by a different general radiologist with 5 years of experience. All measurements were performed in a blinded and randomized manner.

We also performed both CT examinations on 3 patients. The first patient had a case of suspected spondylolisthesis and was scanned with automatic exposure control (tube current modulation) using a noise index of 24, a slice thickness of 5 mm, and a peak tube voltage of 100 kVp in both the supine and upright positions. The second patient had a case of suspected pelvic floor prolapse and was scanned with automatic exposure control using a noise index of 18 and a peak tube voltage of 100 kVp in both the supine and upright positions. The third patient had a case of suspected inguinal hernia and was scanned with automatic exposure control using noise indexes of 15 and 24 and peak tube voltages of 120 and 100 kVp in the supine and upright positions, respectively. For the third patient, 120 kVp CT images in supine position had been previously obtained during routine examination before the patient was enrolled in our study, and thus, we did not take any additional images with the patient in the supine position.

Statistical Analysis

Data are presented as mean ± standard deviation. Differences in the examination time, area and flattening of vessels, and position of the pelvic floor between upright and supine positions were assessed using the Wilcoxon signed-rank test. Differences in age and in deviation of the pelvic floor between men and women were assessed using the Mann-Whitney *U* test. A P value of less than 0.05 (2 sided) was considered significant. Interobserver and intraobserver agreements were evaluated by measuring intraclass correlation coefficients. All data were analyzed using a commercially available software program (SPSS version 24; IBM SPSS, Armonk, NY).

RESULTS

Phantom Study

Both noise characteristics and spatial resolution of upright CT were comparable to those of conventional CT (Fig. 5). The average CT number of upright CT was within the specification range of the Catphan 504 manual, similar to conventional CT (Table 2).

Volunteer Study

The average age of the subjects was 48.4 ± 11.5 years (range, 30–68 years), and their average BMI was 22.5 ± 3.0 kg/m^2 (range, 16.7–30.6 kg/m^2). There was no significant difference in age between women and men (48.4 ± 10.2 vs 48.4 ± 13.0, P = 1.00). Among the

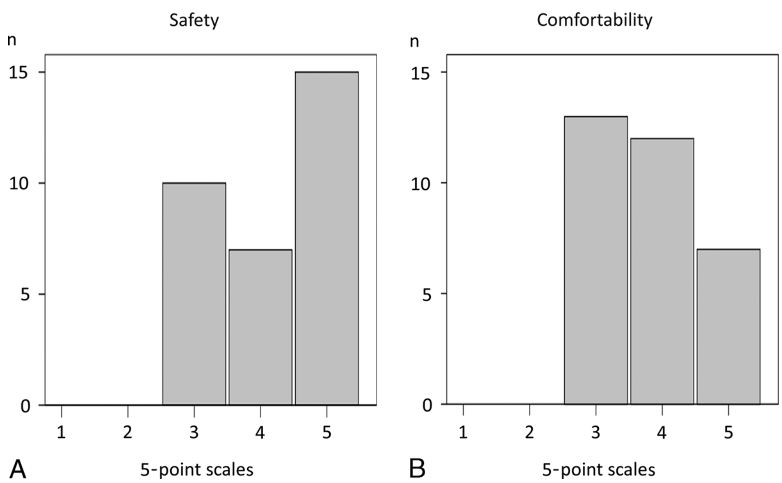

FIGURE 6. Results of the questionnaire survey. The average rating for safety throughout examination (A) was 4.2. The average rating for comfortability throughout examination (B) was 3.8. Scale: 5 = excellent, 4 = good, 3 = fair, 2 = unsatisfactory, 1 = bad.

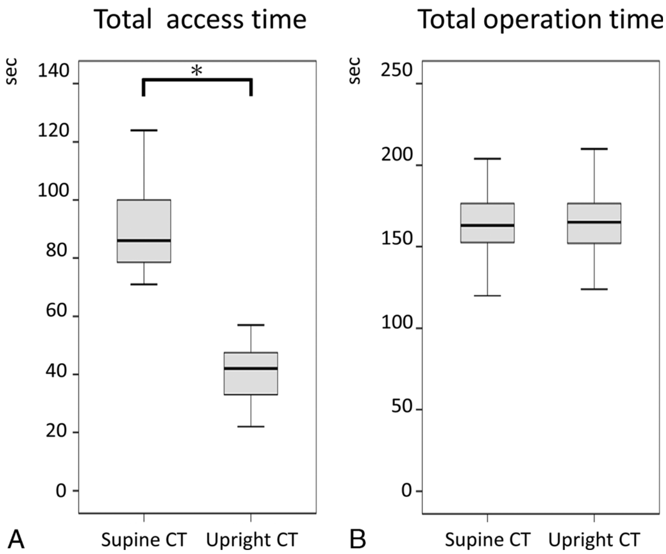

FIGURE 7. Total access time and total operation time. "Total access time" refers to the sum of the entry and exit times. Total access time (A) was significantly shorter in upright CT than in supine CT, while total operation time (B) was similar between the 2. Box plot shows the 5th and 95th (vertical lines), 25th and 75th (Boxes), and 50th (horizontal line) percentile values for total access time or operation time (excluding outliers and extreme values). *$P < 0.001$.

16 women, 9 had given birth and 7 had not. The main scan time was 13.7 ± 0.6 seconds for scans of 833.4 ± 1.5 mm in both supine and upright scans.

The results of the questionnaire survey were that all volunteers answered "yes" regarding stability when using the pole. The average safety rating was 4.2 (15 ratings of 5, 7 ratings of 4, and 10 ratings of 3; Fig. 6A). The average comfortability rating was 3.8 (7 ratings of 5, 12 ratings of 4, and 13 ratings of 3; Fig. 6B).

The total access time was significantly shorter in upright CT than in supine CT (upright: 41 ± 9 seconds vs supine: 91 ± 15 seconds, $P < 0.001$, respectively; Fig. 7, see Supplementary Video 2 (upright CT), Supplemental Digital Content 2, http://links.lww.com/RLI/A474 and Supplementary Video 3 (supine CT) Supplemental Digital Content 3, http://links.lww.com/RLI/A475, which demonstrates that the length of time from entering the room to starting the scan is markedly shortened in upright CT). There was no significant difference in the total operation time between the 2 positions (upright: 167 ± 22 seconds vs supine: 168 ± 31 seconds, $P = 0.736$; Fig. 7).

In the upright position compared with the supine position, the area of the vena cava was significantly smaller by 80% at the SVC (upright: 39.9 ± 17.4 mm^2 vs supine: 195.4 ± 52.2 mm^2, $P < 0.001$) but larger by 37% at the IVC (upright: 346.6 ± 96.9 mm^2 vs supine: 252.5 ± 93.1 mm^2, $P < 0.001$). The degree of flattening was greater by 56% at the SVC (upright: 0.42 ± 0.14 vs supine: 0.27 ± 0.12, $P < 0.001$) but smaller by 58% at the IVC (upright: 0.15 ± 0.08 vs supine: 0.36 ± 0.16, $P < 0.001$). Both were not significantly different at the level of the diaphragm (upright: 428.3 ± 87.9 mm^2 vs supine: 426.1 ± 82.0 mm^2, $P = 0.866$; upright: 0.44 ± 0.08 vs supine: 0.42 ± 0.08, $P = 0.096$; Figs. 8, 9; Table 3). Conversely, the area and degree of flattening of the aorta were not significantly different between CT examinations at all 3 levels (Fig. 8, Table 3).

Both the bladder neck and anorectal junction descended significantly in the standing position compared with the supine position (9.4 ± 6.0 mm and 8.0 ± 5.6 mm, respectively, both $P < 0.001$; Figs. 10, 11; Table 4); these differences remained when men and women were examined separately (both $P < 0.001$; Table 4). The bladder showed greater deviation between the supine and standing positions in women, compared with that in men (12.2 ± 5.2 mm in women vs 6.7 ± 5.6 mm in men, $P = 0.006$); however, there was no significant difference in deviation of the anorectal junction (9.1 ± 5.7 mm in women vs 6.9 ± 5.4 mm in men, $P = 0.196$; Table 4).

Interobserver and intraobserver agreements were substantial in all measurements (0.884–0.999; Tables 3, 4).

Images of Patients

Case 1

A 63-year-old woman presented with a 3-month history of low-back pain and sciatic pain affecting the right leg. She had full strength in her legs and normal sensation to light touch and a pin prick. Her symptoms worsened with standing and walking, and she could not walk more than 100 m without rest. Sagittal and axial CT in the supine position showed spondylolisthesis between the L4 and L5 vertebrae and lumbar foraminal stenosis, which proved more remarkable in the standing position (Fig. 12). This change in the spinal canal space and foramen with posture explained the intermittent claudication with lumbar spondylolisthesis. Due to unstable foraminal stenosis based on her posture, interbody fusion after decompression at L4/5 was performed. She showed complete recovery from her symptoms.

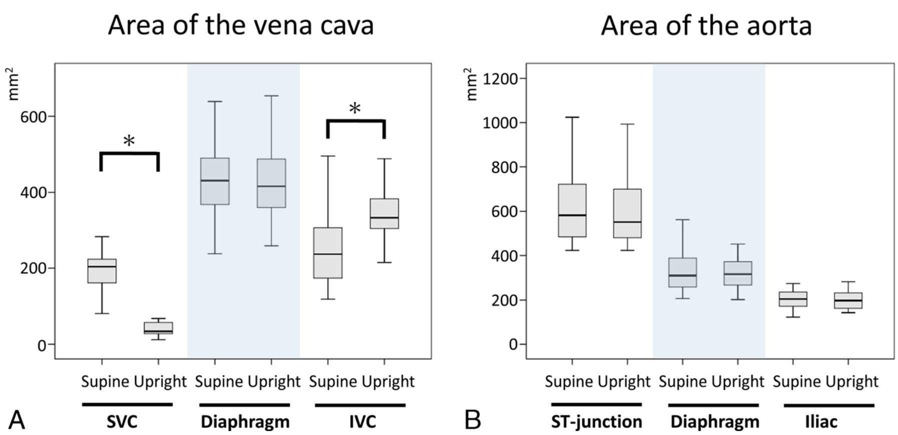

FIGURE 8. Area of vessels. When comparing the upright position with the supine position, the area of the vena cava (A) was smaller at the SVC; the area was not significantly different at the level of the diaphragm; and the area was larger at the iliac bifurcation of IVC. The area of the aorta (B) was similar at all 3 levels. ST indicates sinotubular. Box plot shows the 5th and 95th (vertical lines), 25th and 75th (Boxes), and 50th (horizontal line) percentile values for the area of vena cava and aorta. *$P < 0.001$.

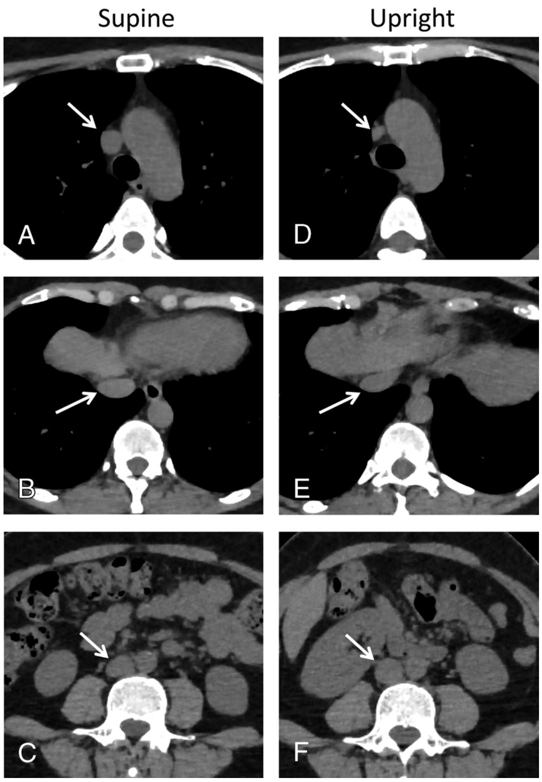

FIGURE 9. Difference of area and flattening of the vena cava at 3 levels. At the superior vena cava, directly below the junction of the bilateral cephalic vein, the area was 143 mm^2 in supine CT (A) and 51 mm^2 in upright CT (D) (64% smaller). The flattening was 0.12 in supine CT (A) and 0.38 in upright CT (D) (3.2-fold increase). At the vena cava, at the level of the diaphragm, the area was 286 mm^2 in supine CT (B) and 259 mm^2 in upright CT (E). The flattening was 0.51 in supine CT (B) and 0.58 in upright CT (E). At the inferior vena cava, directly above the iliac bifurcation, the area was 199 mm^2 in supine CT (C) and 241 mm^2 in upright CT (F) (21% larger). The flattening was 0.3 in supine CT (C) and 0.1 in upright CT (F) (66% decrease).

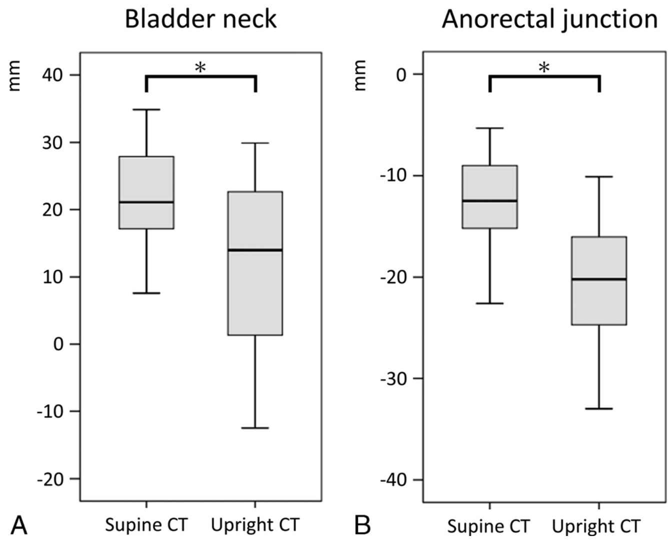

FIGURE 10. Position of pelvic floor. Both bladder neck (A) and anorectal junction (B) descended significantly in the standing position compared with the supine position. Box plot shows the 5th and 95th (vertical lines), 25th and 75th (Boxes), and 50th (horizontal line) percentile values for the position of bladder neck and anorectal junction. *$P < 0.001$.

Case 2

A 75-year-old woman presented with suspected pelvic floor prolapse. The patient had undergone a total abdominal hysterectomy 25 years prior. She came to our hospital with a complaint of genital swelling in the standing position, which had persisted for 5 years. The bladder prolapse was not detected on conventional supine CT but was detected on upright CT (Fig. 13). Based on the findings of upright CT, the patient underwent a tension-free vaginal mesh operation and her swelling was reduced.

Case 3

A 68-year-old man presented with left inguinal swelling and discomfort. Conventional supine CT showed a mild left inguinal hernia that consisted of fat tissue only (Fig. 14A). Upright CT showed more apparent inguinal hernia that consisted of small intestine and fat tissue (Fig. 14B). There was a considerable difference in the size of the hernia orifice between the results of the 2 imaging modalities. The patient underwent inguinal hernia repair and is now symptom free.

DISCUSSION

Cross-sectional imaging in the supine position is useful for the evaluation of organic diseases, such as infectious diseases, cancer, and atherosclerotic disease; for the evaluation of many functional diseases,

TABLE 3. Area and Flattening of Vena Cava and Aorta

	Area on Supine CT, mm^2	Area on Upright CT, mm^2	*P* for Area	Flattening on Supine CT	Flattening on Upright CT	*P* for Flattening	Interobserver/ Intraobserver Agreements for Area on Upright CT	Interobserver/ Intraobserver Agreements for Area on Supine CT
SVC	195.4 ± 52.2	39.9 ± 17.4	<0.001	0.27 ± 0.12	0.42 ± 0.14	<0.001	0.969/0.988	0.946/0.987
Vena cava at the level of diaphragm	426.1 ± 82.0	428.3 ± 87.9	0.866	0.42 ± 0.08	0.44 ± 0.08	0.096	0.969/0.987	0.971/0.991
IVC	252.5 ± 93.1	346.6 ± 96.9	<0.001	0.36 ± 0.16	0.15 ± 0.08	<0.001	0.992/0.997	0.901/0.995
Ascending aorta	608.4 ± 152.9	604.5 ± 157.2	0.358	0.05 ± 0.04	0.03 ± 0.03	0.076	0.997/0.999	0.991/0.996
Aorta at the level of diaphragm	330.3 ± 90.3	327.5 ± 85.5	0.633	0.03 ± 0.02	0.03 ± 0.02	0.254	0.995/0.996	0.991/0.994
Abdominal aorta	202.9 ± 40.9	199.4 ± 38.9	0.074	0.05 ± 0.04	0.05 ± 0.03	0.822	0.949/0.986	0.884/0.994

Flattening: (major axis – minor axis)/major axis of vessels. CT indicates computed tomography; SVC, superior vena cava; IVC, inferior vena cava.

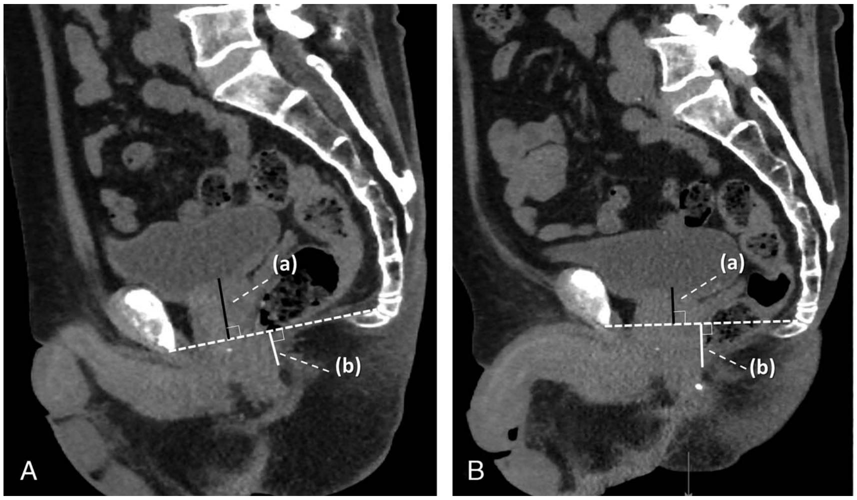

FIGURE 11. Difference in position of the pelvic floor. The distance from bladder neck to PC line (A) was 25 mm in the supine position (A), but 10 mm in the upright position (B) (15 mm descent). The distance from anorectal junction to PC line (B) was 12 mm in the supine position (A), but 20 mm in the upright position (B) (8 mm descent). Both bladder neck and anorectal junction descended significantly in the standing position compared with the supine position. A, From bladder neck to PC line. B, From anorectal junction to PC line. Dotted line indicates PC line (pubococcygeal line); black line, bladder neck; white line, anorectal junction.

cross-sectional imaging in the standing position is necessary. However, imaging in the standing position with a feasible examination time and a sufficient spatial resolution has not yet been available. Thus, both normal control data and patient data have not been well evaluated.

Our phantom study showed that noise characteristics, spatial resolution, and CT numbers of upright CT were comparable to those of conventional supine CT, even when the gantry was arranged in a horizontal position. This indicated that upright CT could be used as a quantitative evaluation tool, in addition to conventional CT.

Our questionnaire survey in the volunteer study showed that all volunteers were subjectively able to maintain stability throughout the acquisition; most also reported feeling safe and comfortable throughout the upright CT examination. Based on these results, the use of pole and a knee-high acrylic wall encircling the body were effective. To support patients who are frail or elderly, a Velcro band can be attached to the pole and loosely wrapped around a patient's body. In this study, the subjects were healthy volunteers and patients who were neither frail nor elderly; thus, we did not use the Velcro band.

Our volunteer study showed that the total access time was significantly shorter in upright CT than in supine CT. The access style of upright CT is the same as that of the plain x-ray examination obtained in a standing position. In this study, we obtained 2 scout views and 1 main scan, all with nearly equal acquisition time. Two scout views were obtained to ensure the accuracy of patient positioning in the upright CT scanner; however, with acclimation, only one view should suffice, which would decrease the total operation time by one third. The benefits of CT over plain x-ray for lung screening have been verified.[25] Thus, in facilities converting from plain x-ray to CT as the main modality for lung screening, upright CT will further enhance the benefits of this conversion. In addition, from a patient's perspective, the reduction of access time may be related to the finding in the questionnaire survey that most volunteers felt comfortable during the upright CT examination.

Our volunteer study found that gravity affected the area of the vena cava differently depending on position; the area was smaller at the SVC, unchanged at the level of the diaphragm, and larger at the

TABLE 4. Position and Deviation of Pelvic Floor

	Measurement on Supine CT, mm	Measurement on Upright CT, mm	The Difference Between Supine CT and Upright CT	*P* for the Difference Between Supine and Upright	*P* for the Difference Between Men and Women	Interobserver/ Intraobserver Agreements for Upright CT Data	Interobserver/ Intraobserver Agreements for Supine CT Data
Distance from bladder neck to PC line							
Total	22.1 ± 6.8	12.6 ± 11.2	9.4 ± 6.0	<0.001		0.993/0.993	0.991/0.964
Men	27.6 ± 4.1	20.9 ± 7.8	6.7 ± 5.6	<0.001	0.006*		
Women	16.6 ± 3.8	4.4 ± 7.3	12.2 ± 5.2	<0.001			
Distance from anorectal junction to PC line							
Total	−12.6 ± 4.4	−20.6 ± 5.9	8.0 ± 5.6	<0.001		0.975/0.939	0.968/0.951
Men	−12.6 ± 3.9	−19.5 ± 6.4	6.9 ± 5.4	<0.001	0.196†		
Women	−12.6 ± 5.0	−21.7 ± 5.2	9.1 ± 5.7	<0.001			

*There is significant difference in the distance from the bladder neck to the PCL between men and women (P = 0.006).

†There is no significant difference in the distance from the anorectal junction to the PCL between men and women (P = 0.196).

CT indicates computed tomography; PC line, pubococcygeal line.

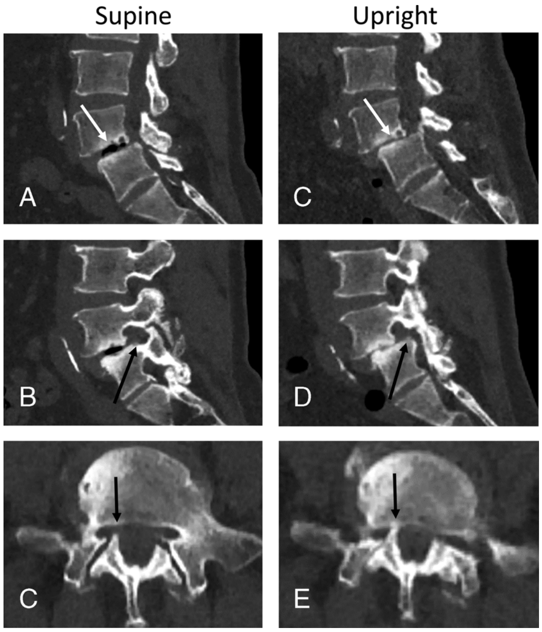

FIGURE 12. A case of spondylolisthesis. Supine CT showed spondylolisthesis between the L4 and L5 vertebrae in the reconstructed midsagittal image (A), and foraminal stenosis in the parasagittal image at the level of foramen (B) and the axial image (C). Upright CT showed a marked increase of stenosis in the spinal canal (D) and foramen (E and F).

IVC in standing position, whereas the area of the aorta remained similar at the 3 different levels. Several studies have evaluated changes of diameter in only the IVC between supine and lateral positions using ultrasonography[26–28]; however, to the best of our knowledge, none has evaluated the change in area of the entire circulation system, including SVC or aorta, between supine and standing positions. The different effects that gravity has on the aorta and vena cava may be due to differences between their vessel walls; the aorta has an elastic wall, whereas the vena cava has a nonelastic wall. The change that we observed in the area of the vena cava is consistent with simulation data that showed low hydrostatic pressure in the upper body and a gradual increase in the lower body.[29] The vein of the upper body in the upright position is considered to be restricted where the static pressure is lower than that in the diaphragm, whereas the vein is considered to be dilated in the lower body where the static pressure is higher. Upright CT might simplify the estimation of the static pressure of the venous system by omitting the need for simulation.

Another simulation study reported that patients with heart failure have high intravenous pressure in the upper body.[30] In daily practice, chest x-ray is used routinely during early evaluation of the enlargement of SVC and IVC borders in such patients. Upright CT can potentially detect slight changes in these vessel volumes, especially SVC. It may be useful in early detection or quantification of the severity of heart failure, compared with plain x-ray. This type of device could help to further elucidate the pathophysiology of the human venous system and could support new concepts in phlebology. Indeed, we have begun studies incorporating enhanced CT in both supine and upright positions to evaluate the effects of gravity on intracranial veins, pulmonary veins, and peripheral veins, and have observed various changes in the venous system.

We also found that the pelvic floor descended in the standing position compared with the supine position. Few studies have evaluated the effects of gravity on the pelvic floor.[10,31] Previous studies using MRI reported that there was no difference in the position of the female pelvic floor between sitting and supine positions,[31] and that straining in the supine position caused descent of the bladder neck (7 mm in men and 10 mm in women) and the anorectal junction (12 mm in men and 11 mm in women).[23] Our study demonstrated that the effect of gravity in the standing position is different from the effects previously reported in the sitting position, and that a similar change due to straining also occurs when standing. Furthermore, the tendency of the bladder neck to descend was more prominent in women than in men. Women are known to be at higher risk of pelvic floor dysfunction.[32,33] Our results show that the female pelvic floor surrounding the bladder is actually lax, which may explain the predominance of urinary incontinence in women.

We described 3 cases of patients with spondylolisthesis, bladder prolapse, and inguinal hernia, respectively, to demonstrate the potential clinical impact of upright CT. All 3 patients described frequent diseases that demonstrated more relevant symptoms or abnormal findings in the standing versus supine position. Spondylolisthesis is a spinal pathology frequently diagnosed in the elderly[34]; pelvic floor prolapse is a common genitourinary disorder affecting close to one third of all women older than the age of 40 years[35,36]; and inguinal hernia is a common condition among men that increases substantially with age.[37] Thus far, although the objective diagnosis and grading of these diseases, as well as assessments of the clinical significance of abnormal findings (in relation to patients' symptoms), are essential for appropriate clinical care and accurate outcome studies, these diseases have not been well evaluated by imaging in the supine position.[38–47] For example, it is reported that supine MRI evaluations of canal stenosis and disk herniation have high false-positive and high false-negative rates, respectively.[39–41] In patients with pelvic organ prolapse, the decision of whether to proceed with a transvaginal or a transabdominal approach depends on which organ is affected and the degree of prolapse, as well as patient and surgeon

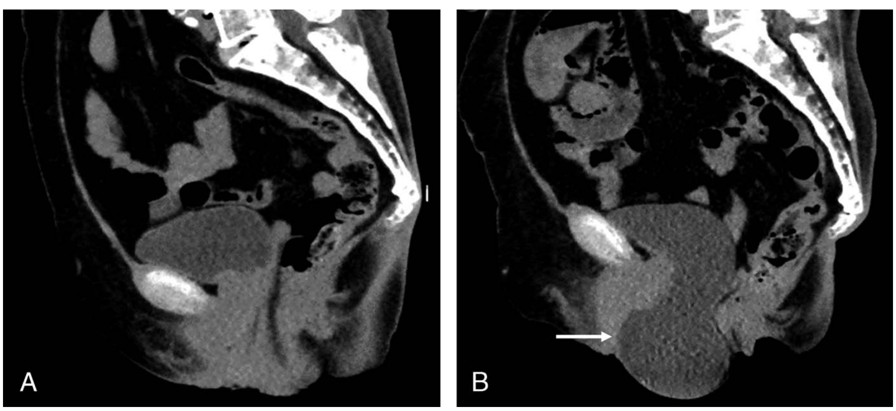

FIGURE 13. A case of pelvic floor prolapse. Bladder prolapse was not detected on conventional supine CT (A), but was detected on upright CT (B, arrow).

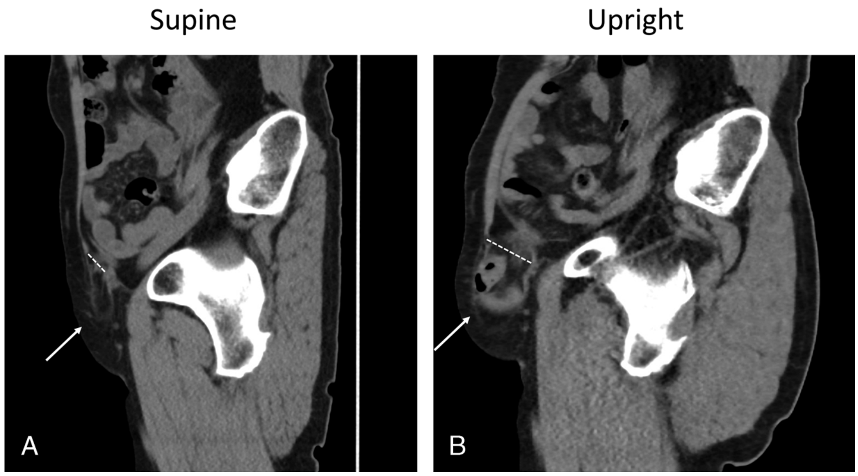

FIGURE 14. A case of inguinal hernia. Conventional supine CT shows mild left inguinal hernia (A, dot line, size of hernia orifice is 16.0 mm), and the hernia content is fat tissue only (A, arrow). Upright CT shows more apparent inguinal hernia (B, dot line, size of hernia orifice is 32.1 mm), and the hernia contents include small intestine and fat tissue (B, arrow).

preference[42]; thus, dynamic supine MRI evaluation was expected to provide integral information in the preoperative assessment. However, there are variations in the sensitivity of dynamic MRI for pelvic organ prolapse,[43,44] and dynamic MRI does not correlate well with clinical findings in patients with middle compartment prolapse.[45] Randomized controlled trials of inguinal hernia have reported that watchful waiting for minimally symptomatic or asymptomatic types is safe.[48–50] However, because inguinal hernias often reduce when affected patients assume the supine position, conventional imaging has not been used for preoperative assessment of inguinal hernia.[46,47] Thus, the evaluations of these diseases largely depend on inspection or integrated interviews by experts, in addition to conventional imaging.

Some studies have reported the use of upright MRI in the evaluation of spondylosis and pelvic floor prolapse,[13,51,52] and the use of prone position CT images in evaluation of inguinal hernia.[53] However, upright MRI with an open configuration has a lower image quality and requires a longer examination time than conventional MRI; moreover, it is often difficult to scan the targeted anatomical structure in the optimal plane.[12,13] The prone position is not a natural posture in daily activities. Although its soft tissue contrast is less than that of MRI, upright CT has a higher spatial resolution with 3-dimensional acquisition of targeted structures and a shorter examination time than upright MRI. Upright CT also can show the daily progression of disease in a manner that differs from that of prone CT. In this study, upright CT scans revealed that the finding of lumbar foraminal stenosis was closely related to symptoms in a patient with spondylolisthesis; moreover, these scans enabled objective diagnosis and grading of patients with bladder prolapse and inguinal hernia, in a manner not apparent when using conventional CT. Thus, the use of upright CT may aid in selecting and formulating the most appropriate treatment matched to the grade of each patient, and may also facilitate more definitive decisions regarding the need or timing for surgery.

There were several limitations in this study. First, the sample size in the volunteer study was small, and it was a single-institution study. A study with a larger sample size and/or a multicenter study is needed to better clarify differences related to age, sex, and birth history. Second, we used unenhanced CT in this study, whereas enhanced CT is generally used for the evaluation of vessels. However, the administration of contrast material may affect circulation status; thus, by using unenhanced scanning, we were able to obtain data that more closely reflected natural vessel size. Third, although we have demonstrated the potential clinical impact in a small subset of patients, further studies with larger patient populations are necessary to confirm the clinical usefulness of upright CT. Such studies are currently underway at our institute. Although all volunteers subjectively reported that stability was good, objective data (eg, spatial resolution in comparisons of upright and supine scans) are necessary to fully evaluate the subjects' stability.

In conclusion, the physical characteristics of upright CT were comparable to those of conventional CT in the phantom study. Upright CT was useful in clarifying the effects of gravity on the entire human body. Gravity differentially affected the volume and shape of the vena cava depending on position, while the aorta volume and shape remained constant regardless of position. This modality offers anatomic visualization of physiologic changes in a large venous system and may allow studies of the effects of position and gravity in cardiovascular manifestations of disease. The pelvic floor descended significantly in the standing position, compared with the supine position. Descent of the bladder neck was more significant in women than in men, which may influence the predominance of urinary incontinence in women. In addition, upright CT clarified abnormal findings of common functional diseases that were not apparent on conventional CT; moreover, it showed the potential for enabling the objective diagnosis and grading of these diseases, as well as determining the clinical significance of abnormal findings in such diseases, which have largely depended on expert experience rather than set guidelines.

ACKNOWLEDGMENTS

The authors thank Akihisa Yamazaki, Koichi Sugisawa, and Kazuya Minamishima for their contribution to the technical supports, and Kyoko Komatsu for her contribution to the manuscript preparation.

REFERENCES

1. Röntgen WC. On a new kind of rays. *Science*. 1896;3:227–231.
2. Kiljunen T, Kaasalainen T, Suomalainen A, et al. Dental cone beam CT: a review. *Phys Med*. 2015;31:844–860.
3. Gang GJ, Zbijewski W, Mahesh M, et al. Image quality and dose for a multisource cone-beam CT extremity scanner. *Med Phys*. 2018;45:144–155.
4. Segal NA, Nevitt MC, Lynch JA, et al. Diagnostic performance of 3D standing CT imaging for detection of knee osteoarthritis features. *Phys Sportsmed*. 2015;43:213–220.
5. Hirschmann A, Buck FM, Fucentese SF, et al. Upright CT of the knee: the effect of weight-bearing on joint alignment. *Eur Radiol*. 2015;25:3398–3404.
6. Zhang JZ, Lintz F, Bernasconi A, et al. 3D biometrics for hindfoot alignment using weightbearing computed tomography. *Foot Ankle Int*. 2019;40:720–726.
7. Benz RM, Harder D, Amsler F, et al. Initial assessment of a prototype 3D cone-beam computed tomography system for imaging of the lumbar spine, evaluating

human cadaveric specimens in the upright position. *Invest Radiol*. 2018;53: 714–719.
8. Hounsfield GN. Computerized transverse axial scanning (tomography). Part 1. Description of system. *Br J Radiol*. 1973;46:1016–1022.
9. Wildermuth S, Zanetti M, Duewell S, et al. Lumbar spine: quantitative and qualitative assessment of positional (upright flexion and extension) MR imaging and myelography. *Radiology*. 1998;207:391–398.
10. Fielding JR, Griffiths DJ, Versi E, et al. MR imaging of pelvic floor continence mechanisms in the supine and sitting positions. *AJR Am J Roentgenol*. 1998; 171:1607–1610.
11. Zamani AA, Moriarty T, Hsu L, et al. Functional MRI of the lumbar spine in erect position in a superconducting open-configuration MR system: preliminary results. *J Magn Reson Imaging*. 1998;8:1329–1333.
12. Botchu R, Bharath A, Davies AM, et al. Current concept in upright spinal MRI. *Eur Spine J*. 2018;27:987–993.
13. Alyas F, Connell D, Saifuddin A. Upright positional MRI of the lumbar spine. *Clin Radiol*. 2008;63:1035–1048.
14. Hara AK, Paden RG, Silva AC, et al. Iterative reconstruction technique for reducing body radiation dose at CT: feasibility study. *AJR Am J Roentgenol*. 2009;193: 764–771.
15. Yamada Y, Jinzaki M, Hosokawa T, et al. Dose reduction in chest CT: comparison of the adaptive iterative dose reduction 3D, adaptive iterative dose reduction, and filtered back projection reconstruction techniques. *Eur J Radiol*. 2012;81: 4185–4195.
16. Yamada Y, Jinzaki M, Tanami Y, et al. Model-based iterative reconstruction technique for ultralow-dose computed tomography of the lung: a pilot study. *Invest Radiol*. 2012;47:482–489.
17. Nickoloff EL. Measurement of the PSF for a CT scanner: appropriate wire diameter and pixel size. *Phys Med Biol*. 1988;33:149–155.
18. Bellesi L, Wyttenbach R, Gaudino D, et al. A simple method for low-contrast detectability, image quality and dose optimisation with CT iterative reconstruction algorithms and model observers. *Eur Radiol Exp*. 2017;1:18.
19. Husby E, Svendsen ED, Andersen HK, et al. 100 days with scans of the same Catphan phantom on the same CT scanner. *J Appl Clin Med Phys*. 2017;18: 224–231.
20. Riederer SJ, Pelc NJ, Chesler DA. The noise power spectrum in computed x-ray tomography. *Phys Med Biol*. 1978;23:446–454.
21. Boedeker KL, Cooper VN, McNitt-Gray MF. Application of the noise power spectrum in modern diagnostic MDCT: part I. Measurement of noise power spectra and noise equivalent quanta. *Phys Med Biol*. 2007;52:4027–4046.
22. Minamishima K, Sugisawa K, Yamada Y, et al. Quantitative and qualitative evaluation of hybrid iterative reconstruction, with and without noise power spectrum models: a phantom study. *J Appl Clin Med Phys*. 2018;19:318–325.
23. Goh V, Halligan S, Kaplan G, et al. Dynamic MR imaging of the pelvic floor in asymptomatic subjects. *AJR Am J Roentgenol*. 2000;174:661–666.
24. Barbaric ZL, Marumoto AK, Raz S. Magnetic resonance imaging of the perineum and pelvic floor. *Top Magn Reson Imaging*. 2001;12:83–92.
25. National Lung Screening Trial Research Team, Aberle DR, Adams AM, et al. Reduced lung-cancer mortality with low-dose computed tomographic screening. *N Engl J Med*. 2011;365:395–409.
26. Grant E, Rendano F, Sevinc E, et al. Normal inferior vena cava: caliber changes observed by dynamic ultrasound. *AJR Am J Roentgenol*. 1980;135:335–338.
27. Nakao S, Come PC, McKay RG, et al. Effects of positional changes on inferior vena caval size and dynamics and correlations with right-sided cardiac pressure. *Am J Cardiol*. 1987;59:125–132.
28. Mookadam F, Warsame TA, Yang HS, et al. Effect of positional changes on inferior vena cava size. *Eur J Echocardiogr*. 2011;12:322–325.
29. van Heusden K, Gisolf J, Stok WJ, et al. Mathematical modeling of gravitational effects on the circulation: importance of the time course of venous pooling and blood volume changes in the lungs. *Am J Physiol Heart Circ Physiol*. 2006; 291:H2152–H2165.
30. Lim E, Chan GS, Dokos S, et al. A cardiovascular mathematical model of graded head-up tilt. *PLoS One*. 2013;8:e77357.
31. Fielding JR, Versi E, Mulkern RV, et al. MR imaging of the female pelvic floor in the supine and upright positions. *J Magn Reson Imaging*. 1996;6:961–963.
32. Bitti GT, Argiolas GM, Ballicu N, et al. Pelvic floor failure: MR imaging evaluation of anatomic and functional abnormalities. *Radiographics*. 2014;34:429–448.
33. MacLennan AH, Taylor AW, Wilson DH, et al. The prevalence of pelvic floor disorders and their relationship to gender, age, parity and mode of delivery. *BJOG*. 2000;107:1460–1470.
34. Iguchi T, Wakami T, Kurihara A, et al. Lumbar multilevel degenerative spondylolisthesis: radiological evaluation and factors related to anterolisthesis and retrolisthesis. *J Spinal Disord Tech*. 2002;15:93–99.
35. Jelovsek JE, Maher C, Barber MD. Pelvic organ prolapse. *Lancet*. 2007;369: 1027–1038.
36. Olsen AL, Smith VJ, Bergstrom JO, et al. Epidemiology of surgically managed pelvic organ prolapse and urinary incontinence. *Obstet Gynecol*. 1997;89: 501–506.
37. Ruhl CE, Everhart JE. Risk factors for inguinal hernia among adults in the US population. *Am J Epidemiol*. 2007;165:1154–1161.
38. Segebarth B, Kurd MF, Haug PH, et al. Routine upright imaging for evaluating degenerative lumbar stenosis: incidence of degenerative spondylolisthesis missed on supine MRI. *J Spinal Disord Tech*. 2015;28:394–397.
39. Kent DL, Haynor DR, Larson EB, et al. Diagnosis of lumbar spinal stenosis in adults: a metaanalysis of the accuracy of CT, MR, and myelography. *AJR Am J Roentgenol*. 1992;158:1135–1144.
40. Weishaupt D, Zanetti M, Hodler J, et al. MR imaging of the lumbar spine: disk extrusion and sequestration, nerve root compression, endplate abnormalities and osteoarthritis of the facet joints are rare in asymptomatic volunteers. *Radiology*. 1998;209:661–666.
41. Stadnik TW, Lee RR, Coen HL, et al. Annular tears and disk herniation: prevalence and contrast enhancement on MR images in the absence of low back pain or sciatica. *Radiology*. 1998;206:49–55.
42. Kobashi KC. Evaluation and management of women with urinary incontinence and pelvic prolapse. In: Wein AJ, Kavoussi LR, Partin AW, et al, eds. *Campbell-Walsh Urology*. 11th ed. Philadelphia, PA: Elsevier; 2016.
43. Gousse AE, Barbaric ZL, Safir MH, et al. Dynamic half Fourier acquisition, single shot turbo spin-echo magnetic resonance imaging for evaluating the female pelvis. *J Urol*. 2000;164:1606–1613.
44. Deval B, Vulierme MP, Poilpot S, et al. Imaging pelvic floor prolapse. *J Gynecol Obstet Biol Reprod (Paris)*. 2003;32:22–29.
45. Cortes E, Reid WM, Singh K, et al. Clinical examination and dynamic magnetic resonance imaging in vaginal vault prolapse. *Obstet Gynecol*. 2004;103:41–46.
46. Fitzgibbons RJ, Quinn TH, Krishnamurty D. Abdominal wall hernias. In: Greenfield LJ, ed. *Surgery*. 6th ed. Philadelphia, PA: Wolters Kluwer Health; 2016.
47. Suzuki S, Furui S, Okinaga K, et al. Differentiation of femoral versus inguinal hernia: CT findings. *AJR Am J Roentgenol*. 2007;189:W78–W83.
48. Fitzgibbons RJ, Giobbie-Hurder A, Gibbs JO, et al. Watchful waiting vs repair of inguinal hernia in minimally symptomatic men: a randomized clinical trial. *JAMA*. 2006;295:285–292.
49. O'Dwyer PJ, Norrie J, Alani A, et al. Observation or operation for patients with an asymptomatic inguinal hernia: a randomized clinical trial. *Ann Surg*. 2006;244: 167–173.
50. HerniaSurge Group. International guidelines for groin hernia management. *Hernia*. 2018;22:1–165.
51. Kubosch D, Vicari M, Siller A, et al. The lumbar spine as a dynamic structure depicted in upright MRI. *Medicine (Baltimore)*. 2015;94:e1299.
52. Abdulaziz M, Kavanagh A, Stothers L, et al. Relevance of open magnetic resonance imaging position (sitting and standing) to quantify pelvic organ prolapse in women. *Can Urol Assoc J*. 2018;12:E453–E460.
53. Miyaki A, Yamaguchi K, Kishibe S, et al. Diagnosis of inguinal hernia by prone- vs. supine-position computed tomography. *Hernia*. 2017;21:705–713.